Application of image visual characterization and soft feature selection in Content-Based Image Retrieval

Kambiz Jarrah[a], Matthew Kyan[b], Ivan Lee[a], and Ling Guan[a]

[a]Multimedia Research Laboratory, Ryerson University, Toronto, Canada
[b]School of Electrical and Information Systems Engineering, University of Sydney, Australia

ABSTRACT

Fourier descriptors (FFT) and Hu's seven moment invariants (HSMI) are among the most popular shape-based image descriptors and have been used in various applications, such as recognition, indexing, and retrieval. In this work, we propose to use the invariance properties of Hu's seven moment invariants, as shape feature descriptors, for relevance identification in content-based image retrieval (CBIR) systems. The purpose of relevance identification is to find a collection of images that are statistically similar to, or match with, an original query image from within a large visual database. An automatic relevance identification module in the search engine is structured around an unsupervised learning algorithm, the self-organizing tree map (SOTM). In this paper we also proposed a new ranking function in the structure of the SOTM that exponentially ranks the retrieved images based on their similarities with respect to the query image. Furthermore, we propose to extend our studies to optimize the contribution of individual feature descriptors for enhancing the retrieval results. The proposed CBIR system is compatible with the different architectures of other CBIR systems in terms of its ability to adapt to different similarity matching algorithms for relevance identification purposes, whilst offering flexibility of choice for alternative optimization and weight estimation techniques. Experimental results demonstrate the satisfactory performance of the proposed CBIR system.

Keywords: content-based image retrieval (CBIR), self-organizing tree map (SOTM), soft feature selection, optimization.

1. INTRODUCTION

With the development of the internet, visual information has been widely used in engineering and scientific applications. Images and video are being captured and categorized in large databases. Therefore, it is extremely important to develop efficient techniques to characterize, search, and retrieve digital images in large visual digital libraries. Capturing all aspects of characteristics of the human visual system is an important, but currently impossible task in designing effective CBIR systems. Therefore, finding a set of feature descriptors that effectively represent the image content becomes an important research area in CBIR.

One important goal of image retrieval is characterizing and recognizing images based on their visual content, regardless of their size and orientation. To achieve this goal, the extracted image features should have properties invariant against image transformations. Although Fourier descriptors are boundary-based image descriptors, they are not directly invariant to image transformations. On the other hand, Hu's seven moment invariants are region-based image descriptors and have these invariance properties by their very nature[1].

In the past[3], we developed an automatic method based on an unsupervised learning approach using a combination of a Multi-Class and Two-Class self-organizing tree map (SOTM). In that work, image shapes were characterized by Fourier descriptors. Although Fourier descriptors have low computational complexity, they are unable to characterize disjoint image shapes. In this paper, the effectiveness of Hu's seven moment invariants in characterizing and quantifying shape features of the objects in images is further investigated. The importance of individual feature descriptors through the notion of automatic feature weighting in the process of automatic relevance identification is also studied in this work. Previously, in the reinforcement learning algorithm of the Multi-Class SOTM, we had used a pre-defined ranking function that was inversely proportional to the ranking of the feature vectors at relevance feedback iterations regardless of their actual similarities[3]. In this paper, we extended our study to define an exponential ranking function that is capable

Multimedia Content Analysis, Management, and Retrieval 2006,
edited by Edward Y. Chang, Alan Hanjalic, Nicu Sebe, Proc. of SPIE-IS&T Electronic Imaging,
SPIE Vol. 6073, 607310, © 2006 SPIE-IS&T · 0277-786X/06/$15

of ranking the feature vectors based on their similarities with regard to query features. We are able to demonstrate that our approach has resulted in a more accurate and more satisfactory retrieval performance.

The rest of the paper is organized as follows: Section 2 provides an introduction to our proposed method in extracting the shape feature using Hu's seven moment invariants. The automatic image retrieval system is then described in section 3 along with the theory behind the automatic relevance identification using SOTM. We conclude this paper in sections 4 and 5 by demonstrating and discussing our experimental results.

2. SHAPE FEATURE EXTRACTION USING HU'S SEVEN MOMENT INVARIANTS

In 1961, Hu[4] first introduced a method for visual patterns and character recognition, independent of position, size, and orientation, based upon two-dimensional moment invariants defined in terms of Riemann integrals. As he explained, the zero-order and first-order moments represent the total image power and can be used to locate the centroid of the density distribution function; whereas the second-order moments characterize the size and orientation of the image. On the other hand, the low-order moments contain the most information regarding to shape, size, and orientation of an image[5].

These moments can not be directly used for characterizing the shape of objects and they must be normalized in such a way that invariance properties can be established. Invariance to position of an object in an image can be achieved by using the central moments of an image whereas scale and contrast invariance can be achieved through normalized central moments[4, 5].

Using different combinations of the normalized central moments, η_{ij}, based on the theory of algebraic invariants, Hu introduced seven moments[4, 5]:

$$
\begin{aligned}
\vartheta_1 &= \eta_{20} + \eta_{02} \\
\vartheta_2 &= (\eta_{20} - \eta_{02})^2 + 4\eta_{11}^2 \\
\vartheta_3 &= (\eta_{30} - 3\eta_{12})^2 + (3\eta_{21} - \eta_{03})^2 \\
\vartheta_4 &= (\eta_{30} + \eta_{12})^2 + (\eta_{21} + \eta_{03})^2 \\
\vartheta_5 &= (\eta_{30} - 3\eta_{12})(\eta_{30} + \eta_{12})\left[(\eta_{30} + \eta_{12})^2 - 3(\eta_{21} + \eta_{03})^2\right] \\
&\quad + (3\eta_{21} - \eta_{03})(\eta_{21} + \eta_{03})\left[3(\eta_{30} + \eta_{12})^2 - (\eta_{21} + \eta_{03})^2\right] \\
\vartheta_6 &= (\eta_{20} - \eta_{02})\left[(\eta_{30} + \eta_{12})^2 - (\eta_{21} + \eta_{03})^2\right] + 4\eta_{11}(\eta_{30} + \eta_{12})(\eta_{21} + \eta_{03}) \\
\vartheta_7 &= (3\eta_{21} - \eta_{03})(\eta_{30} + \eta_{12})\left[(\eta_{30} + \eta_{12})^2 - 3(\eta_{21} + \eta_{03})^2\right] \\
&\quad + (3\eta_{21} - \eta_{30})(\eta_{21} + \eta_{03})\left[3(\eta_{30} + \eta_{12})^2 - (\eta_{21} + \eta_{03})^2\right].
\end{aligned}
\qquad (1)^*
$$

In this paper, the HSMI shape descriptors were extracted by converting the colour images into binary segmented images and then extracting the shape parameters from those segmented images using Eq. 1. The binary image segmentation was performed through the following processes, as shown in Fig. 1:

1. Resize the input image to a uniform number of pixels;
2. Convert the image to a gray scale image;
3. Create a binary image using a proper threshold value;
4. Detect edges of the original image using Canny filters;
5. Perform a flood-fill operation on background pixels of the binary image in (4);
6. Subtract the filled image region in (5) from the edge image in (4) and dilate the resulting image;
7. Add the dilated image to the gray scale image;
8. Create a binary image from the image in (7);
9. Perform morphological operations to clean up resulting image in (8);
10. Perform the logic AND operation on image in (9) and (3) and resize the resulting image to its original size;

* Interested readers are referred to references 4 and 5 for more detailed derivations of these equations.

11. Label connected objects in binary image in (10);
12. Measure a set of properties for each labeled region; and
13. Select region of interests within the image in (12).

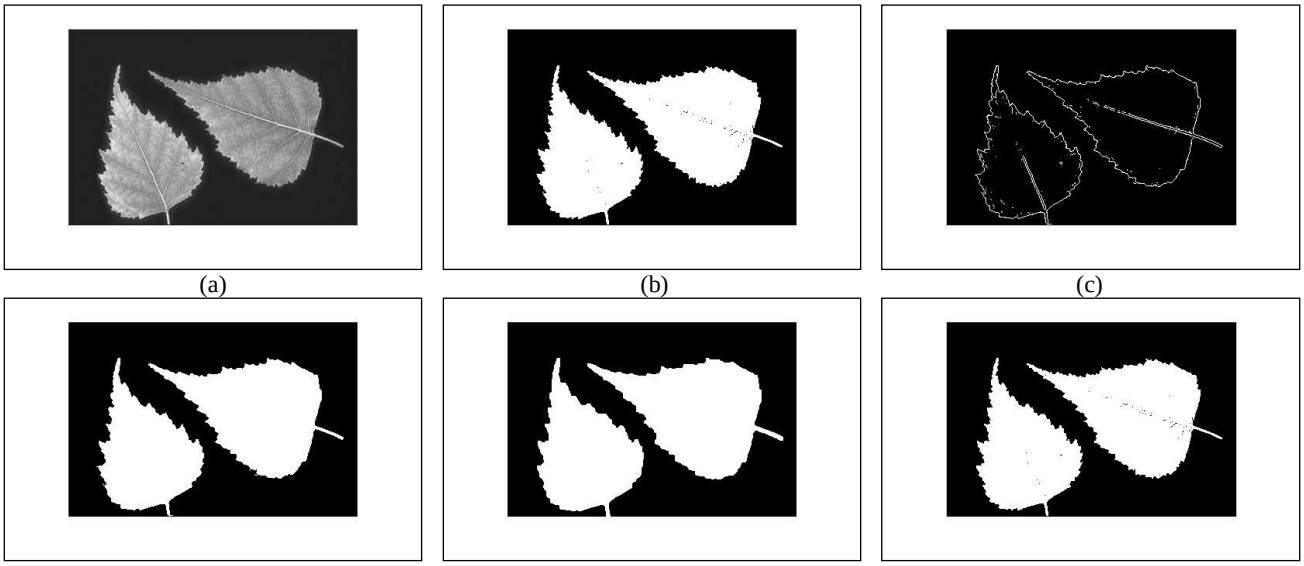

Figure 1: Binary image segmentation. From the above process: (a) Steps 1 and 2, (b) Step 3, (c) Step 4, (d) Steps 5 to 8, (e) Steps 8 and 9, and (f) Steps 10 to 13.

As we can see, the binary segmentation aims to preserve important information by characterizing image objects and differentiating them from their redundant background information. After binary segmentation, the resulting uniform object regions are passed through the process of HSMI feature calculations.

3. AUTOMATIC RELEVANCE FEEDBACK

The block diagram of the proposed automatic CBIR system is illustrated in the "*Automatic Search*" block of Fig. 2. The basic idea of the automatic CBIR system is to apply an unsupervised machine learning algorithm to perform the decision making required in identifying the relevance of retrieved images, instead of involving human users directly in the feedback loop[2].

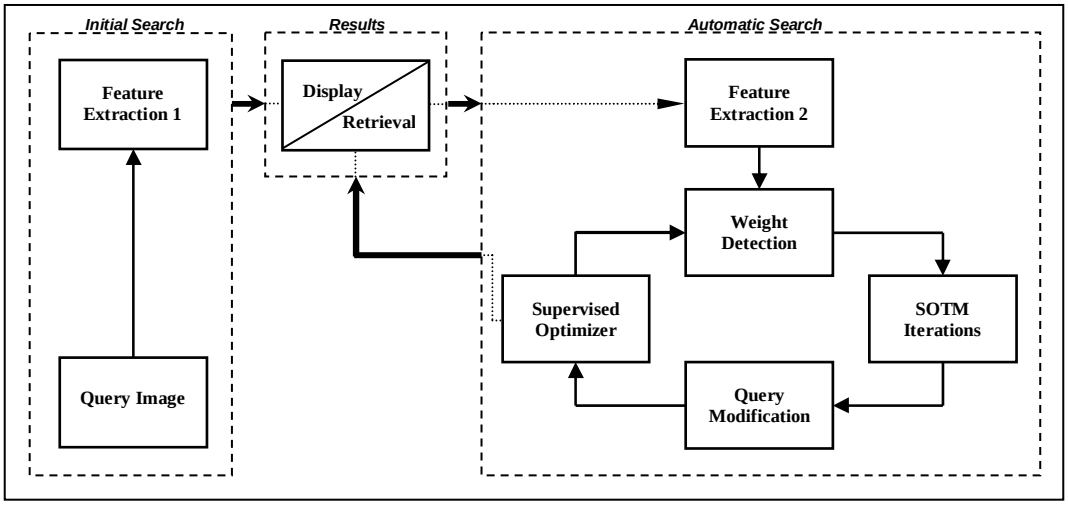

Figure 2: Proposed CBIR System (System-A.)

Fig. 2 has two feature extraction blocks, which function differently. In *Feature Extraction module 1* of the *"initial search"* block[3], features of reasonable quality, which can be efficiently computed, are extracted for fast retrieval. Accuracy of retrieval is not that important at this stage since we are dealing with a high volume of images; therefore the features used in the first module have low computational cost and are thus more desirable. These features are then compared to other feature vectors in the database, based on predefined distance measurements, and the most similar images (in a relative sense) are displayed back to the user through the *"Results"* block. Subsequently, upon user's request, control of the system is transferred to the *"automatic search"* module, which operates completely independent of the previous blocks.

At this stage, similarity measurements and query adjustments are performed using new feature descriptors extracted in *Feature Extraction module 2*. In this module, features of higher quality are extracted from the retrieved images for automatic relevance identification. Computation of those features could be intensive, but since such features are only computed for the few retrieved images, they become feasible at this stage. Table 1 summarizes the features used in the both feature extraction modules of Fig. 2.

Feature Extraction Module 1	Feature Dimension	Feature Extraction Module 2	Feature Dimension
FFT Shape Descriptors	1 × 10	HSMI Shape Descriptors	1 × 7
Colour Moment	1 × 9	Colour Moment	1 × 9
Colour Histogram	1 × 48	Colour Histogram	1 × 48
Wavelet Moment†	1 × 20	Gabor Descriptors	1 × 48

Table 1: Content descriptors used in different modules of the CBIR System-A.

In the *"automatic search"* module, the system is firstly transferred to the distance measurement phase to identify relatively top 25 similar images. In *Weight Detection* module different weights are then applied to the query feature vectors (i.e. colour, shape, and texture) and response of the system is subsequently quantified by measuring the ability of each of the five *SOTM iterations* in correctly classifying the selected images in relevant and irrelevant image classes (see section 3.1.) A new query, based upon the selected images from the previous iterations, is then selected to substantially represent the relevant class through the *Query Modification* module[3]. The system response, in terms of retrieval accuracy, is next assessed by the user in the *Supervised Optimizer* block. The final retrieved images are then displayed back to the user.

3.1 Multi-Class Self-Organizing Tree Map (SOTM)

SOTM is an unsupervised machine learning algorithm which is effective in minimizing human involvement in relevance identification. The Self Organizing Tree Map is an extension of the Self-Organizing Map (SOM), which is used for the purpose of unsupervised data clustering[8-10]. The SOTM essentially classifies input vectors into several different clusters (classes), specifying the centroid of each. This polythetic approach assumes that there may be multiple irrelevant clusters, each likely to be different not only to the relevant (query) class, but also from each other. Capturing a single relevant class and multiple irrelevant classes allows for a more non-linear partitioning of images into both relevant and irrelevant groupings. Once identified, information from the relevant cluster may be used to modify the query so as to better encapsulate the spread of relevant images in any subsequent search iteration (see Fig. 3).

An SOTM mapping begins with an isolated root node (representing a single cluster centroid) and builds through a competitive learning process by dynamically creating new nodes (centroids) as more input vectors are presented to the SOTM. This process is achieved by evaluating a similarity measure between all nodes currently formed in the SOTM mapping, and the next input vector. If a vector is encountered whose similarity exceeds some threshold function (i.e. is significantly different from all nodes in the current SOTM map, a new node (centroid) is generated. The new node is attached as a leaf node of its closest representation in the current SOTM mapping, thus over time, a tree structure evolves[11]. If the root node is initialized as the query vector, any new centroids so discovered typically represent groups of statistically irrelevant images[7]. The growth of the SOTM can be biased via a ranking function to learn more from

† Extracted from mean, μ, and standard deviation, σ, of three-level wavelet transform applied on an image.

input vectors deemed to be similar to the query itself, and little from images far from the query[10]. This promotes the generation of multiple irrelevant classes, whilst maintaining necessary plasticity in the relevant class.

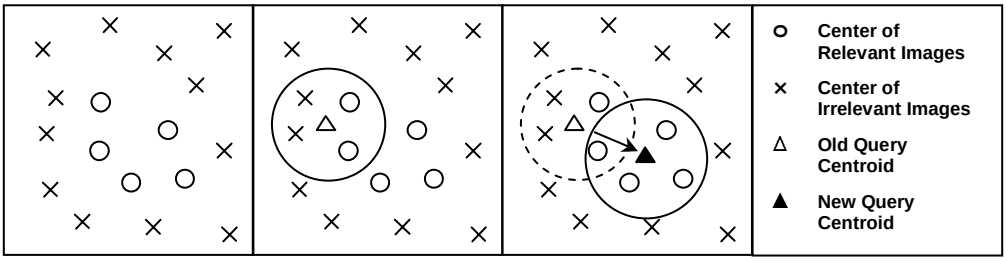

Figure 3: Polythetic Clustering Approach using Multi-Class SOTM - from left to right: original dataset, clustering of relevant class using SOTM at the first iteration, updated clustering using SOTM at the subsequent iterations.

The SOTM algorithm is summarized in the following steps:

Initialization: Choose a root node, $\{\mathbf{w}_i\}_{j=1}^{J}$, from the available set of input vectors, $\{\mathbf{x}_k\}_{k=1}^{K}$, in a random manner. *J* is the total number of centroids (initially set to 1).

Similarity Matching: Randomly select a new data point **x**, and find the winning centroid, j^*, by using the minimum distance Euclidean criterion in Eq. 2.

$$\mathbf{w}_{j^*}(t) = \arg\min_j \left\| \mathbf{x}(t) - \mathbf{w}_j(t) \right\|, \qquad j = 1,2,\ldots,\boldsymbol{J} \ . \tag{2}$$

Updating: *If* $\left\| \mathbf{x}(t) - \mathbf{w}_{j^*} \right\| \le H(t)$, where *H(t)* is the hierarchy function used to control the levels of the tree and decreases in time according to $H(t+1) = \lambda H(t)$, where λ is the threshold decreasing constant and $0 < \lambda < 1$ *then* assign x(t) to the j[th] centroid, and adjust the synaptic vector according to the reinforce learning rule:

$$\mathbf{w}_{j^*}(t+1) = \mathbf{w}_{j^*}(t) + \alpha(t)\beta(\mathbf{z},\mathbf{x},t)\left[\mathbf{x}(t) - \mathbf{w}_{j^*}(t)\right], \tag{3}$$

where $\alpha(t)$ is the learning rate, which decreases monotonically with time, $\alpha(t) = \alpha(t)/(\alpha(t) + 0.5)$, $0 \le \alpha(t) \le 1$; and $\beta(\mathbf{z},\mathbf{x},t)$ is an exponential ranking function, which measures the similarity between the query feature vector, **z**, and the feature vector, **x**, from the subset of images retrieved at the relevance feedback iteration of the previous search operation (Eq. 4). A High value of $\beta(\mathbf{z},\mathbf{x},t)$ indicates a high relevance of the feature vector with respect to the associated query feature at the time *t*.

$$\beta(\mathbf{z},\mathbf{x},t) = \sum_{i=1}^{P} G_i(x_i - z_i) = \sum_{i=1}^{P} \exp\left(-\frac{(x_i - z_i)^2}{2\sigma_i^2} \right), \tag{4}$$

where P is the total number of features, $\sigma_i = \eta \max_i |x_i - z_i|$ is a tuning parameter that distributes the measure of similarity over the inherent spread in the feature vectors, and η is an additional factor to ensure a large output for $\beta(\mathbf{z},\mathbf{x},t)$ in Eq. 4. *Else* form a new centroid node starting with **x** and increment j^* by 1.

Continuation*:* Continue with similarity matching stage until no noticeable changes in the feature map are observed.

The key difference compared with the previous studies[2, 3] is the addition of the function $\beta(\mathbf{z},\mathbf{x},t)$ that helps group irrelevant images into several clusters by not only a predefined ranking metric but also by taking an exponential similarity measurements between the query feature vector and the feature vector of the retrieved images.

To be consistent with previous studies[2, 3], a combination of Two-Class and Multi-Class SOTM is also used in this work. As it was previously explained[3], the Multi-Class SOTM is very effective in classifying images in large databases whereas the Two-Class SOTM is very capable of classifying images in a small database.

3.2 Weight Estimation and Optimizer Modules

The purpose of feature weighting is to de-emphasize certain features that do not necessarily contribute significant information about how relevant an image is in the retrieval process, thereby achieving a form of soft feature selection. Throughout this work, the importance of the feature weighting contributing to the SOTM classification and its affect on improving the retrieval results and overall performance of the system was studied. It was observed that assigning weights for the individual features by assessment with an appropriate performance measurement algorithm can increase the performance of the CBIR system significantly.

The processes of weight estimation and supervised optimizer modules are combined in the following steps:

1. Let $\mathbf{z} = [x_c, x_t, x_s]$ represent the query feature vector constructed from colour, texture, and shape features respectively (Table 1);
2. Define new colour, $[Cw_n]_{n=1}^{N}$, and new texture, $[Tw_m]_{m=1}^{M}$, feature weights and create a new query feature vector, $\mathbf{z}_{New}$, where $\mathbf{z}_{New} = [(Cw_n \times x_c), (Tw_m \times x_t), (1 \times x_s)]$. In above equations M and N are arbitrary user defined boundaries for the weights;
3. Investigate the behavior of each of the five iterations of SOTM to the presented feature weights, R_i, and create a set of retrieval results, R_{ij}, where $i = 1,\ldots,5$ and $j = 1,\ldots, (M \times N)$. The SOTM performance measurements, R_i s, are computed by the user based on number of retrieved images that fall into the query class in each iteration of weight adjustments, j;
4. Detect the most accurate retrieval results, V_j, where $V_j = \mathbf{max}_i |[R_{ij}]_{i=1}^{5}|$. If $V_j > V_{j-1}$, the best weights are Cw_n and Tw_m and the best retrieval rate is $RR = V_j$ in the j^{th} iteration;
5. Increase m by one and go back to step 2 until $m=M$;
6. Increase n by one and go back to step 2 until $n=N$.

Please note that in all these iterations the shape feature weight is kept constant since one of our objectives is to compare the performance of systems A and B (Figs. 2 and 4) in presence of different shape descriptors in improving the retrieval results regardless of the imposed feature weights.

Even though the above process requires human supervision, the amount of required human-computer interactions is less than would be required if used in conjunction with the manual steps needed in typical relevance feedback type CBIR systems[2]. In our system, the initial manual steps are shifted away from providing relevance feedback as the SOTM assumes this role (automatic clustering to achieve query modification). Furthermore, human participation may be eliminated completely, if the assessment of 'good performance' supplied by the user in the weight estimation process above, is replaced by some form of fitness or cost function (a factor currently under study). What will be clear from this study, is that consideration of a weight estimation module that tailors weightings to an individual image query, has a profound impact on the retrieval results. Ultimately suggesting that features contributing to what makes one class of images perceptually similar, are not likely to be the same set of features contributing to what makes another class of images perceptually similar. If this final weight estimation module can be fully automated, the subjectivity introduced by a user's interpretation of the query may be alleviated.

.

4. EXPERIMENTAL RESULTS

A number of experiments were conducted to compare the behavior of the "*Automatic Search*" module of the CBIR engine in Fig. 2, using HSMI as the shape feature verses the one in Fig 4, using Fourier descriptors as the shape descriptor[3]. The simulations were carried out using a subset of the Corel image database consisting of nearly 5100 Joint Photographer's Expert Group (JPEG) colour images, covering a wide range of real-life photos, from 51 different

categories. Each category consisted of 100 visually associated objects to simplify the measurements of the retrieval accuracy during the experiments. The statistical results were calculated from the retrieval of 102 query images, two from each class. In the simulations, a total of 16 most relevant images were retrieved to evaluate the performance of the retrieval. The performance was then measured in terms of Retrieval Rate (*RR*).

Feature Types in System-A	Feature Dimension	Feature Types in System-B	Feature Dimension
HSMI Shape Descriptors	***1 × 7***	***FFT Shape Descriptors***	***1 × 10***
Colour Moment	1 × 9	Colour Moment	1 × 9
Colour Histogram	1 × 48	Colour Histogram	1 × 48
Gabor Descriptors	1 × 48	Gabor Descriptors	1 × 48

Table 2: Content descriptors used in the *"Automatic Search"* module of CBIR Systems A and B.

Table 2 illustrates an overview on the features used in feature extraction modules of *"Automatic Search"* block of systems A and B. Fourier descriptors provide shape features of reasonable quality in retrieval; whereas, Hu's seven moment invariants (HSMI) represent shape features of high quality given that they are more reliable in terms of representing disjoint sections of objects in the images. Since one of the objectives is to test the effectiveness of the shape features in automatic CBIR, we used the same colour and texture features for both systems in the experiments.

In particular, colour histograms and colour moment descriptors in the HSV and RGB colour spaces were computed as the colour descriptors, and Gabor wavelet features were calculated from mean, μ, and standard deviation, σ, of Gabor filtered images as the texture descriptors. Fourier shape parameters were extracted using Sobel filters for the purpose of edge detection due to their low computational cost. The resulting edge parameters were then converted from Cartesian coordinate to the polar coordinate and the Fast Fourier Transform (FFT) was then applied and the low frequency components are extracted to form a 10-dimensional feature vector. HSMI shape parameters were extracted by converting the colour images into binary segmented images and then extracting the shape parameters from those segmented images using the technique described in section 2.

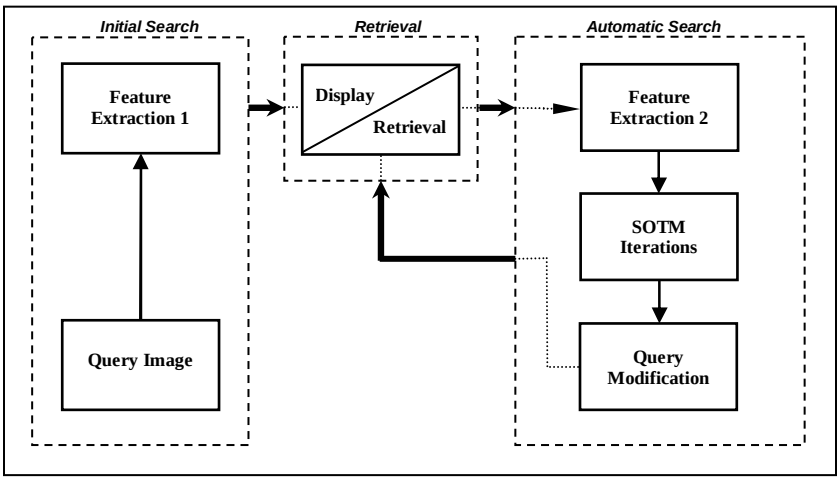

Figure 4: CBIR System[3] (System-B.)

The graphs in Fig. 5 indicate the system performance (*RR*) based on the number of retrieved images for each of the selected queries; for instance, there are 57 tested query images, out of 102 total queries, that result in 100% system accuracy in Fig. 5a. In other words, there are 27 tested query images result in 100% retrieval rate in Fig. 5b. Table 3 illustrates another interpretation of the graphs in Fig. 5.

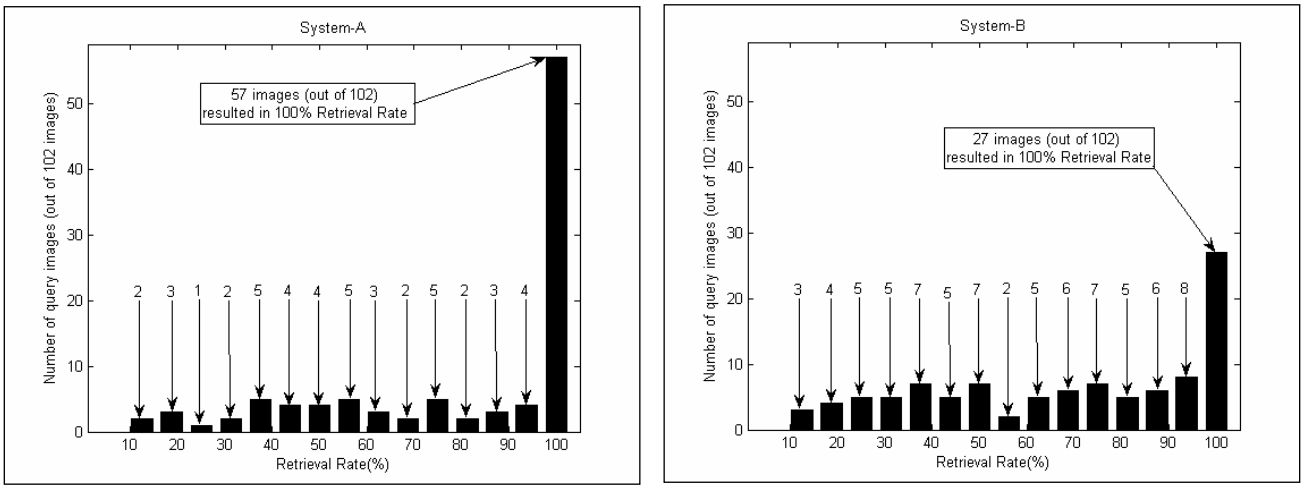

(a) (b)

Figure 5: Experimental results using the automatic CBIR systems A and B. Assigned values on each arrow represent a total number of query images, out of total 102, that resulted in their respective Retrieval Rate.

The experimental results are summarized in Table 4. The average retrieval rate was calculated by dividing the total number of images that correctly retrieved by the total possible correct retrieval. By looking at these results, it is apparent that the combination of the improved unsupervised learning algorithm, the more robust shape features, and the supervised weight detection/optimizer scheme can enhance the retrieval results significantly.

Retrieval Rate (RR)	Total Number of Retrieved Images (out of 102)	
	System-A	System-B
RR ≤ 50%	21	36
50% < RR ≤ 75%	15	20
75% < RR ≤ 100%	66	46

Table 3: Another interpretation of Fig. 5; each row represents the total number of query images that result in different Retrieval Rate. As we can see, higher numbers of images result in acceptable retrieval rate in the CBIR system-A than system-B. The results were taken out of total 102 selected images.

Type of CBIR System	Average Retrieval Rate
System - A	80.51%
System - B	66.32%

Table 4: Average retrieval rate using the CBIR systems A and B. The results show the superiority of the proposed technique over the previous method[3].

5. CONCLUSIONS

In this paper we demonstrated an improved framework for automatic image retrieval systems. The effectiveness of unsupervised learning in minimizing human involvement in image retrieval was clearly shown. It was shown that HSMIs are capable of capturing the shape characteristics in relevance identification in automatic CBIR systems.

In addition, it was illustrated that the process of automatic weight detection, as a form of soft feature selection, for the content descriptors (colour and texture) and the user-based optimizer for sensing and detecting the maximum relevance can enhance the search engine's performance significantly. Although having a set of invariant shape descriptors, used in this system, can effectively characterize the images, it was discovered that the weight detection and optimizer had a significant role in improving the performance results. This is because of the ability of these modules to identify the peak retrieval performance of different query images with respect to the applied feature weights regardless of the nature of shape features.

A draw back of this system is the human involvement in the process of weight estimation and optimization. As it was explained, the amount of required human involvement is less than that in relevance feedback type CBIR systems, since human participation is not required in similarity matching and decision making stages of this system. Here the SOTM assumes this responsibility. The only task the user fulfills then is in assessing the performance in terms of retrieved images falling into the query class with respect to the imposed query feature weights. As such, this shift in user interaction has allowed for a system that constructs a more flexible model of the query feature's class – one that gives emphasis to features deemed important in terms of perceptual similarity with respect to that particular query. This was reflected in the significantly improved retrieval accuracies reported in this work. As such, future research efforts are being directed to the development of a fully automated weight estimation and optimization module, to minimize and alleviate any subjectivity introduced by user interaction.

REFERENCES

1. Qing Chen, Emil Petriu, Xiaoli Yang, *"A Comparative Study of Fourier Descriptors and Hu's Seven Moment Invariants for Image Recognition,"* IEEE CCECE 2004- CCGEI 2004, Niagara Falls, pp. 103-106, May 2004

2. P. Muneesawang and L. Guan, *"Minimizing user interaction by automatic and semiautomatic relevance feedback for image retrieval,"* Proc. IEEE Int. Conf. on Image Processing, Rochester, USA, pp. 601-604, vol.2, Sept. 2002

3. Kambiz Jarrah, Paisarn Muneesawang, Ivan Lee, and Ling Guan, *"Minimizing Human-Machine Interactions in Automatic Image Retrieval,"* IEEE CCECE 2004- CCGEI 2004, Niagara Falls, pp. 1589-1592, May 2004

4. M. K. Hu, *"Visual pattern recognition by moment invariants,"* IRE Trans. Inf. Theory, Vol.IT-8, pp.179-187, February 1962

5. S. Paschalakis and P. Lee, *"Pattern recognition in gray level images using moment based invariant features,"* IEE Conference Publication on Image Processing and its Applications, No.465, pp.245-249, 1999.

6. P. Muneesawang, H. S. Wong, J. Lay, and L. Guan, *"Learning and Adaptive Characterization of Visual Contents in Image Retrieval Systems,"* Chapter 11 in Y.H. Hu and J.-N. Hwang, Handbook of Neural Network Signal Processing, CRC Press LLC, 2001

7. Ivan Lee, Paisarn Muneesawang, and Ling Guan, *"Automatic Relevance Feedback for Distributed Content-Based Image Retrieval,"* ICGST International Journal on Graphics, Vision and Image Processing, Vol. V4, 2005

8. H.S. Kong, L. Guan, *"Self-Organizing Tree Map for Eliminating Impulse Noise with Random Intensity distributions,"* Journal of Electronic Imaging 7(1), 36-44, January 1998.

9. J. Randall, L. Guan, X. Zhang, and W. Li, *"Investigations of the Self-Organizing Tree Map,"* in Proc. Int. Conf. Neural Inform. Processing, Vol. 2, Perth, Australia, Nov. 1999, pp. 724-728

10. P. Muneesawang, and L. Guan, *"Automatic Machine Interactions For Content-Based Image Retrieval Using a Self-Organizing Tree Map Architecture,"* IEEE Tran on Neural Networks, Vol. 13, No. 4, July 2002, pp. 821-834

11. M. Kyan, L. Guan and S. Liss, *"Dynamic feature fusion in the self organizing tree map – applied to the segmentation of biofilm images"*, Proceedings of the International Joint Conference on Neural Networks. July 31-August 4, 2005, Montreal, Canada.